PHYSICAL REVIEW D VOLUME 7, NUMBER 7 1 APRIL 1973

Electroproduction and Photoabsorption in a Model of Higher Baryon Couplings

Sudhir K. Sood and A. N. Mitra
Department of Physics and Astrophysics, University of Delhi, Delhi-7, India
(Received 20 July 1972)

We have studied the two related problems of inelastic e^--N scattering and the total photoabsorption cross section in a relativistic SU(6) × O(3) model of higher baryon couplings developed over the last few years. The hypothesis of duality is incorporated for both these photonic processes by summing over an infinite sequence of s-channel resonances, the facility for which is provided in this model of $\bar{B}_L B(P, V)$ couplings through a simple structure of the form factor for the supermultiplet transition ($L^P \to 0^+$) and a "Regge universality" condition on the "reduced" coupling constants. A slight variant of this form factor, which has been applied successfully to several two-body processes recently, is found to give rather good fits to the resonance-production region of inelastic e^--N scattering over a wide range of input data. The difference ($\Delta\sigma_T$) of the total photoabsorption cross section on the proton and the neutron targets is also reproduced quite accurately over the whole range of available data. For these two processes, the higher-spin ($J = L + \frac{1}{2}$, $J = L + \frac{3}{2}$) states are found to produce dominant contributions over those of the lower-spin ($J = L - \frac{1}{2}$) states. A comparison of this pattern with a corresponding one operative for the evaluation of electromagnetic masses within this model prompts us to infer almost a "causal" relationship between the positive value of $\Delta\sigma_T$ on the one hand and the traditional negative value of ($\delta m_p - \delta m_n$) on the other. However, an important shortcoming of this model is its inability to reproduce the scaling region of deep-inelastic e^--N scattering for very high incident electron energies ($\epsilon > 10$ GeV). This is presumably because of the absence in this model of a mechanism for the inclusion of daughter trajectories, whose contributions are expected to be progressively more important as the energy is increased.

I. INTRODUCTION

The role of resonances in different high-energy processes has been increasingly felt over the years since finite-energy sum rules (FESR)[1,2] and duality[3,4] were proposed. We have gone a long way from the earliest application of these principles to the area of π-N scattering,[3] and the duality spirit now pervades more complicated processes involving vector and electromagnetic interactions.[5] The most obvious applications of electromagnetic couplings of resonances are photoproduction processes and the inelastic e^--N scattering, which provide direct experimental tests of these couplings at lightlike and spacelike distances, respectively. Of these, the study of inelastic e^--N scattering has generally been classified into two regions: (i) the production of resonances and (ii) deep-inelastic scattering. The investigations in these two areas have, till very recent times, been carried out independently of each other, despite the facilities for correlation provided by duality. In the same vein, the techniques employed for these purposes have been very different. Thus, whereas in the resonance region the techniques of the nonrelativistic quark model have been employed,[6] the deep-inelastic region, on the other hand, has been characterized by the natural language of "scaling,"[7] a concrete realization of which is achieved through Feynman's parton model.[8]

It is only in more recent times that some serious attempts have been made to bridge the gap between the low- and high-energy regions through a greater reliance on duality principles. A recent analysis of Bloom and Gilman[9] suggests that the scaling property which has traditionally been thought to be the exclusive reserve of large-energy-transfer processes probably applies equally well to the region of resonances. They have further argued in favor of a strong nondiffractive part ($I=1$) of the virtual-photon–nucleon scattering amplitude which accounts for a substantial part of the observed behavior of inelastic e^--N scattering. The physical importance of this result derives its strength from the mode of arrival at this conclusion, viz., from a direct analysis of the data in terms of fairly general principles rather than through any specific model.

Calculations of electroproduction and deep-inelastic scattering using more specific relativistic models have also been carried out in recent times. Examples of such approaches are the relativistic quark model of Feynman *et al.*[10] and the model of Domokos *et al.* for resonance production.[11] While the former has been applied strictly to the resonance region, the Domokos model represents a more serious attempt to push the resonance contributions to the "scaling region" through a statistical ansatz called "equipartition" of channels bearing on the number of open channels for the decay of a resonance of given energy. Both these models are, of course, characterized by the appearance of *ad hoc* form factors which presumably carry a significant burden of dynamics. The important conclusion that emerges from such models is that it is not unphysical to expect a significant part of the inelastic e^--N scattering amplitude to be saturated by direct-channel resonances. Similar conclusions have been reached by other authors as well.[12]

As a closely related process to inelastic e^--N scattering, the total photoabsorption cross section offers another important item of comparison of such models with experiment. Indeed a careful comparison of the roles of the different ingredients of the model for the twin processes of electroproduction and photoabsorption could throw a significant light on the role of s-channel resonances in producing the experimental features.

The present paper represents an attempt to study the twin problems of inelastic e^--N scattering and the $I=1$ part of real γ-N scattering via direct-channel resonances in terms of a relativistic model of higher baryon couplings that has been developed over the last few years at Delhi University. The purpose of this study is twofold. At a qualitative level, it is designed to test the working of duality for some important photonic processes as several others[5] have done on different premises. At a more quantitative level the study of these two processes is undertaken to provide another nontrivial example in the series of several systematic applications of the above model that have been pursued recently. The model, which has so far been applied with a fair amount of success to (i) decays of resonances,[13,14] (ii) γ production of π, η,[15,16] and (iii) V-meson production in $(\pi, K)N$ collisions,[17] is strongly reminiscent of $\mathrm{SU}(6)_W$ features[18,19] with the additional assumption of a phenomenological form factor corresponding to a complete supermultiplet ($L^P \to 0^+$) transition in the language of $\mathrm{SU}(6)\times\mathrm{O}(3)$. Several different versions of this form factor within a certain class having the general structure x^l (where x has the dimension of an inverse momentum and l is the partial wave for the P-meson coupling) have been proposed[20,21] so as to conform, in varying degrees, to some broad requirements of symmetry, asymptotics, and universality for reduced coupling constants. Of these, the one which has so far shown the greatest promise for fitting the data for several processes simultaneously gives a nontrivial form factor even for the nucleon ($L=0$).[21] A minor variant of this model will be considered specifically for the present investigation of inelastic e^--N scattering and γ-N scattering.

A particular interest in γ-N scattering lies in the observation that while γ-p scattering is *experimentally* higher than γ-n scattering,[9] the *opposite* seems to happen when the two-photon lines join up to make a single electromagnetic self-energy loop, since the electromagnetic mass of n is higher than that of p. This apparent anomaly (?) raises an interesting question of whether these two phenomena are (or are not) at all compatible with each other. A plausible explanation for $\delta m_n - \delta m_p > 0$ was recently offered[22] within this model in terms of a simple mechanism of $\gamma_5\gamma_\mu$-type (axial-vector, or "magnetic-charge"-type) coupling which is available for all $J=L-\frac{1}{2}$ states ($L \geq 1$) and whose contributions more than offset the "wrong sign" contributions arising from $J=L+\frac{1}{2}$ states (governed mainly by "electric-charge"-type couplings). It is therefore of interest to ask what role this mechanism plays in γ-N scattering where the "electric-charge"-type coupling must dominate the "magnetic-charge" type if the experimental data are to be understood at all. One of the objects of this investigation is to offer a clarification of this apparent contradiction within the framework of our model of higher baryon couplings.

The layout of the paper is as follows. In Sec. II, we summarize the assumptions on (i) the baryon spectrum and their total widths, (ii) the structure of various types of electromagnetic couplings together with the requirements of gauge invariance, and (iii) the structure of the form factors. Section III gives the formalism for both the inelastic e^--N scattering and (real) forward Compton scattering in the isovector state. Following the classic treatment of the kinematics of inelastic e^--N scattering by Bjorken and Walecka,[23] we give, in the first part of this section, the formulas for the double differential cross section and the contributions to the structure functions W_1 and W_2 arising from various resonances. The method of calculations for the evaluation of individual resonance contributions to this process is indicated for one particular type of vector coupling which, hopefully, is sufficiently illustrative of the different features of the inelastic e^--N amplitudes within the model. The second part of this section describes the corresponding algebra on real Compton scattering in the isovector state. Section IV deals with the problems of extrapolation off the mass shells of the photon and the resonances. Section V gives the results of our calculations for the inelastic e^--N scattering (covering both the resonance and the continuum regions) and the $I=1$ part of photoabsorption cross section, together with a comparison with the experimental data as well as with other contemporary models. Section VI summarizes our main conclusions.

II. THE BASIC INGREDIENTS OF THE MODEL

Most of the material of this section including, in particular, the electromagnetic coupling scheme has already been discussed extensively elsewhere.[15,24] It is only for the sake of a sufficiently self-contained description that we outline here the essential features for the purpose of this investigation.

A. Masses and Widths of Resonances (B_L)

While we assume that $S=0$ baryon spectra have straight-line trajectories as most authors do, we also assume that the only supermultiplets that exist are the following:

$$[\underline{56}, 2l^+], \quad [\underline{70}, (2l+1)^-].$$

Several arguments (experimental and theoretical) have been offered for these in the literature,[25,26] but the scope of this paper does not warrant a detailed discussion about them.

For the masses of the N- and Δ-type states, we use empirical relations of the type $M_L{}^2 \simeq aL+b$, where $a \approx 1.0$ GeV^2 represents the universal slope for all trajectories, and the values of b for different trajectories can be calculated by inserting the mass of the leading particle. Analogous empirical relations for the total widths of these states have been conjectured by several authors,[11] a sufficiently accurate representation being[27]

$$\text{for } N\text{-type states,} \quad \Gamma_n = \Gamma_0 + 0.20(M_n - M_0),$$

$$\text{for } \Delta\text{-type states,} \quad \Gamma_n = \Gamma_0 + 0.16(M_n - M_0),$$

where Γ_n and M_n are the total width and the mass of the nth recurrence on the trajectory and Γ_0 and M_0 are the corresponding quantities for the leading particle of the trajectory.

In Table I we list the values of Γ_0 and M_0 for the trajectories that make dominant contributions to the processes we are considering, viz., N_α, N_γ, and N_β'' (Ref. 28) among N-type states and Δ_δ and Δ_α among Δ-type states.

TABLE I. List of the total widths (Γ_0) and masses (M_0) of the leading particles of the towers that make dominant contributions in our calculations.

Tower	Leading particle J^P	M_0 (GeV)	Γ_0 (GeV)
N_α	$N(938)$ $\frac{1}{2}^+$	0.938	0.0
N_γ	$D_{13}(1520)$ $\frac{3}{2}^-$	1.525	0.105
N''_β	$D_{15}(1675)$ $\frac{5}{2}^-$	1.675	0.240
Δ_δ	$P_{33}(1238)$ $\frac{3}{2}^+$	1.238	0.120
Δ_α	$F_{35}(1880)$ $\frac{5}{2}^+$	1.880	0.250

B. The Couplings

The general relativistic couplings in our model are of the multiderivative type connecting Rarita-Schwinger fields with Dirac fields characterized by (i) the SU(6)×O(3) factors and (ii) an over-all form factor governing each supermultiplet transition. The structures of $\overline{B}_L BP$ and $\overline{B}_L BV$ couplings have been connected via the requirement of "partial symmetry" at the level of $\overline{Q}(P, V)Q$ interactions.[24,29] We shall use the latest version of this coupling scheme (the β scheme) in which the entire $(L+1)$-wave coupling structures are parametrized through the direct term in $\overline{Q}MQ$ coupling and the entire $(L-1)$-wave interaction via the quark-recoil term alone.[15] The possible types of $\overline{B}_L BV$ couplings which are generated in this model are as follows:

$$A \equiv \overline{\psi}^{L+1/2}_{\mu_1\cdots\mu_L}(P)(i\sigma_{\mu\nu}k_\nu)k_{\mu_1}\cdots k_{\mu_L}V_\mu\psi(p) \qquad (L+1) \text{ wave},$$

$$B \equiv \overline{\psi}^{L+1/2}_{\mu_1\cdots\mu_L}(P)(i m_V\gamma_\mu)k_{\mu_1}\cdots k_{\mu_L}V_\mu\psi(p) \qquad L \text{ wave},$$

$$C \equiv \overline{\psi}^{L-1/2}_{\mu_2\cdots\mu_L}(P)(i\gamma_5\gamma_\mu)k_{\mu_2}\cdots k_{\mu_L}V_\mu\psi(p) \qquad (L-1) \text{ wave}, \tag{2.1}$$

$$D \equiv \overline{\psi}^{L+3/2}_{\lambda\mu_1\cdots\mu_L}(P)(i\epsilon_{\lambda\nu\mu\sigma}k_\nu V_\mu\gamma_\sigma)k_{\mu_1}\cdots k_{\mu_L}\psi(p) \qquad (L+1) \text{ wave (also valid for } J=L-\tfrac{1}{2}),$$

$$E \equiv \overline{\psi}^{L+1/2}_{\mu\mu_2\cdots\mu_L}(P)V_\mu k_{\mu_2}\cdots k_{\mu_L}\psi(p) \quad (L-1) \text{ wave}.$$

Here P, p, and k are the four-momenta of the resonance, proton, and vector meson, respectively. V_μ and m_V are the polarization vector and the mass of the vector meson concerned.[30] Of the above coupling types, A, B, and D arise out of the direct term while C and E are generated by the recoil term only.

In Table II, we bring together all the $\overline{B}_L BV$ couplings to both the N- and Δ-type states along with the appropriate SU(6)×O(3) factors.

The electromagnetic interaction is now included through the vector-meson dominance (VMD)[31] assumption where the "two point" vertex is given by

TABLE II. List of $\bar{B}_L BV$ couplings of N-type and Δ-type states along with the appropriate SU(6) × O(3) factors. The couplings to neutral ρ and ω mesons are listed separately. The letters A–E account quantitatively for the factors indicated in Eqs. (2.1).

A. N-type states

Coupling to	$[\underline{56}, (L+\frac{1}{2})]$ N_α	$[\underline{70}, (L+\frac{1}{2})_d]$ N_γ	$[\underline{70}, (L+\frac{1}{2})_q]$ N'_γ
ρ	$-\frac{5}{3}A\tau_3 + B\tau_3 + \frac{5}{3}\left(\frac{L}{2L+1}\right)^{1/2} E\tau_3$	$-\frac{2}{3}\sqrt{2}\,A\tau_3 + \sqrt{2}B\tau_3 + \frac{2}{3}\sqrt{2}\,E\tau_3$	$\frac{1}{\sqrt{3}}\left(\frac{L}{2L+3}\right)^{1/2} A\tau_3$
ω	$-A + 3B + \left(\frac{L}{2L+1}\right)^{1/2} E$	$-\sqrt{2}A + \sqrt{2}\left(\frac{L}{2L+1}\right)^{1/2} E$	$-\left(\frac{3L}{2L+3}\right)^{1/2} A$

Coupling to	$[\underline{70}, (L-\frac{1}{2})_d]$ N'_β	$[\underline{70}, (L+\frac{3}{2})_q]$ N''_β	$[\underline{56}, (L-\frac{1}{2})]$ N_δ	$[\underline{70}, (L-\frac{1}{2})_q]$ N_β
ρ	$\frac{2}{3}\sqrt{2}\,\tau_3\left[\left(\frac{L+1}{2L+1}\right)C - \left(\frac{L-1}{2L+1}\right)D\right]$	$\frac{1}{\sqrt{3}}D\tau_3$	$\frac{5}{3}\tau_3\left[\left(\frac{L+1}{2L+1}\right)C - \left(\frac{L-1}{2L+1}\right)D\right]$	0
ω	$\sqrt{2}\left[\left(\frac{L+1}{2L+1}\right)C - \left(\frac{L-1}{2L+3}\right)D\right]$	$-\sqrt{3}D$	$\left[\left(\frac{L+1}{2L+1}\right)C - \left(\frac{L-1}{2L+1}\right)D\right]$	0

B. Δ-type states

Coupling to	$[\underline{56}, (L+\frac{3}{2})]$ Δ_δ	$[\underline{56}, (L+\frac{1}{2})]$ Δ_α	$[\underline{70}, (L+\frac{1}{2})]$ Δ_γ	$[\underline{70}, (L-\frac{1}{2})]$ Δ_β
ρ	$\frac{4}{\sqrt{3}}D$	$\frac{4}{\sqrt{3}}\left(\frac{L+1}{2L+3}\right)^{1/2} A$	$\frac{1}{\sqrt{3}}(A+3B) - \frac{1}{\sqrt{3}}\left(\frac{L}{2L+1}\right)^{1/2} E$	$-\frac{1}{\sqrt{3}}\left(\frac{L+1}{2L+1}\right)C + \frac{1}{\sqrt{3}}\left(\frac{L-1}{2L+1}\right)D$

$$\mathcal{L}_{\text{e.m.}} = j_\mu^{\text{e.m.}} A_\mu ,$$
$$e^{-1} g_\rho j_\mu^{\text{e.m.}} = m_\rho^{\,2} \rho_\mu^0 + \tfrac{1}{3} m_\rho^{\,2} \omega_\mu - \tfrac{1}{3}\sqrt{2}\,\phi_\mu m_\phi m_\rho , \tag{2.2}$$

where we have taken $m_\rho \approx m_\omega$ and $g_\rho^{\,2}/4\pi = g_{\rho\pi\pi}^{\;\;2}/4\pi = 2.9$, as predicted by the form factor described below. The (small) ϕ term will henceforth be neglected.

The result of putting the γ-V and $\bar{B}_L BV$ vertices together is to produce effective $\bar{B}_L B\gamma$ vertices (valid for *both* real and virtual photon interactions) of the form

$$\left(\frac{m_\rho^{\,2}}{m_\rho^{\,2} + k^2}\right) \frac{e}{g_\rho} \left(j_\mu^{(\rho)} \tau_3 + \tfrac{1}{3} j_\mu^{(\omega)}\right) A_\mu , \tag{2.3}$$

where the currents $j_\mu^{(\rho,\omega)}$ are the coefficients of the corresponding vector mesons (ρ_μ or ω_μ) in the various coupling Lagrangians described in (2.1) and Table II.

Regarding the question of gauge invariance of the above couplings, it is clear that the types A and D are explicitly gauge-invariant. The other couplings can be made formally gauge-invariant through the following modifications:

$$B \text{ type:} \quad i\gamma_\mu V_\mu \to \left(i\gamma_\mu - \frac{(P+p)_\mu}{M+m}\right) V_\mu ,$$
$$C \text{ type:} \quad i\gamma_5\gamma_\mu V_\mu \to \left(i\gamma_5\gamma_\mu - \frac{(P+p)_\mu}{M-m}\gamma_5\right) V_\mu , \tag{2.4}$$
$$E \text{ type:} \quad \psi_\mu V_\mu \to \psi_\mu V_\mu - \frac{\psi\cdot k}{k^2} k_\mu V_\mu ,$$

where M and m are the masses of the produced resonance and the target nucleon, respectively.

C. Form Factors

The couplings given above now need to be multiplied by form factors which have been parametrized separately for $(L\pm 1)$ waves and will be denoted by $f_{LJ}^{(\pm)}$. Out of several varieties[20,21] that have been discussed in this connection, we pick up one which was suggested (on purely empirical grounds) by Chaudhury *et al.*[21] and which seems to work best on the whole for several processes simultaneously.[15,16,32] We consider here a slight variant of this structure, and this, when all particles are on the mass shell, is

$$f_{LJ}^{(+)}=\left(\frac{2(Mm)^{1/2}S_F(J)^{1/4}}{M^2+m^2-\mu^2}\right)^{L+1}\left(\frac{\mu}{m_\pi}\right)^{1/2}c_L^{(+)},$$

$$f_{LJ}^{(-)}=\left(\frac{2(Mm)^{1/2}S_F(J)^{1/4}}{M^2+m^2-\mu^2}\right)^{L}\left(\frac{\mu}{m_\pi}\right)^{1/2}\frac{m_A{}^2}{m_{A_1}}c_1^{(-)}. \tag{2.5}$$

Here S_F is a sort of "scale" factor whose magnitude has been adjusted from the ratio of $\Delta\to N\pi$ decays of two successive Regge recurrences, to 1.26; μ is the mass of the appropriate meson (P or V); m_A and m_{A_1} are the masses of the axial-vector counterpart of the P (or V) meson and the A_1 meson, respectively. The values of the reduced coupling constants are given by[21]

$$C_{2l}^{(\pm)}=C_2^{(\pm)},\quad C_2^{(+)}=C_0^{(+)},\quad C_{2l+1}^{(\pm)}=C_1^{(\pm)},$$
$$S_F{}^2C_0^{(+)2}/4\pi=2.05,\quad C_1^{(+)2}/4\pi=1.5, \tag{2.6}$$
$$C_1^{(-)2}/4\pi=0.05,\quad C_1^{(+)}/C_1^{(-)}=C_2^{(+)}/C_2^{(-)}.$$

The modification which (2.5) represents over the corresponding one of Ref. 21 lies in the form of the denominator which is now $(M^2+m^2-\mu^2)$, instead of the original $(M^2+m^2+\mu^2)$ which was symmetrical in all the masses. This modification, which makes little difference as long as the "meson" is on its mass shell, would therefore leave essentially unaltered the results of most decay calculations as well as those of photoproduction[15] and πN collisions.[32] The motivation for this modification is mainly theoretical, viz., (i) it helps avoid the (ugly) problem of falling mass spectra[33] and (ii) it allows a mathematically more meaningful extrapolation of the form factor off the meson mass shell (or equivalently the photon mass shell) via the prescription $\mu^2\to -k^2$ since the structure $M^2+m^2+k^2$ is free from the danger of a sign flip in the denominator for sufficiently large k^2, a problem which would arise if the extrapolation in the mass of the quantum were made from the expression $M^2+m^2+\mu^2$.[34] Additional problems of extrapolation off the mass shell are discussed in Sec. IV.

III. FORMALISM

We summarize here the necessary algebraic formalism (including the details of normalization) for the two processes of electroproduction and total photoabsorption on the nucleon.

A. Inelastic e^--N Scattering

The Feynman diagram for this process is shown in Fig. 1. An electron of energy ϵ and mass m_e scatters off a nucleon of four-momentum p_μ and mass m at an angle θ in the laboratory frame and with final energy ϵ', producing a final state of four-momentum P_μ by means of exchange of a single

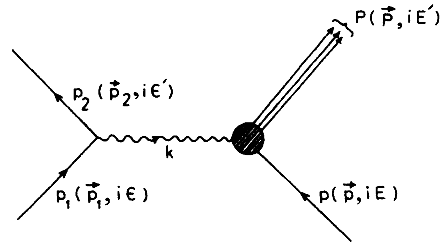

FIG. 1. Kinematics of the inelastic e^--N scattering.

photon of four-momentum k_μ. When only the final electron is observed, everything can be expressed in terms of two Lorentz invariants which we choose for our discussion to be the squared four-momentum transfer $k^2\,[=4\epsilon\epsilon'\sin^2(\frac{1}{2}\theta)]$ and the invariant missing mass W given by

$$-P^2=W^2$$
$$=m^2-k^2+2m\nu, \tag{3.1}$$

where $\nu\ (=\epsilon-\epsilon')$ is the electron energy loss.

The differential cross section for the production of a single final-state resonance of mass M_i is expressible as[23]

$$\frac{d\sigma_i}{d\Omega'}=\frac{\alpha^2}{e^2}\,\frac{1}{4\epsilon^2\sin^2(\frac{1}{2}\theta)}\left(\frac{\cos^2(\frac{1}{2}\theta)}{2m+4\epsilon\sin^2(\frac{1}{2}\theta)}\right)\times M_i[\,\xi_2(M_i{}^2,k^2)+2\tan^2(\tfrac{1}{2}\theta)\xi_1(M_i{}^2,k^2)], \tag{3.2}$$

where α is the fine-structure constant and ξ_1 and ξ_2 are related to the well-known structure functions W_1 and W_2 (Ref. 35) by the equation

$$W_{\mu\nu}=\frac{1}{2e^2}\int\frac{d^3P}{E'}\,(mM_i)(\xi_{\mu\nu})\delta^4(P-p-k),$$
$$\xi_{\mu\nu}=\xi_1\left(\delta_{\mu\nu}-\frac{k_\mu k_\nu}{k^2}\right) \tag{3.3}$$
$$+\xi_2\frac{1}{m^2}\left(p_\mu-\frac{p\cdot k}{k^2}k_\mu\right)\left(p_\nu-\frac{p\cdot k}{k^2}k_\nu\right).$$

The scalars ξ_1 and ξ_2 provide the most direct language for evaluating the contributions of individual resonances to the inelastic e^--N scattering cross sections. As an illustration, we outline in Appendix A an explicit calculation of ξ_1 and ξ_2 for a particular type of coupling (type A).

The double-differential cross section for this process, which is deduced from (3.2) as

$$\frac{d^2\sigma}{d\Omega'd\epsilon'}=\sum_{\text{resonances }(i)}\left(\frac{d\sigma_i}{d\Omega'}\right)\delta\left(\epsilon'-\frac{m^2+2m\epsilon-M_i{}^2}{2m+4\epsilon\sin^2(\frac{1}{2}\theta)}\right), \tag{3.4}$$

must now take account of the finite width of the resonances. We do this in the standard manner of replacing a δ function by a Breit-Wigner structure.

Since several versions of this replacement are available,[27] we specify our prescription through the ansatz

$$\pi\delta(P^2+M^2)=\left(\frac{M_i\Gamma_i}{(M_i^2-W^2)+M_i^2\Gamma_i^2}\right)$$
$$\rightarrow\frac{1}{2M_i}\left(\frac{\frac{1}{2}\Gamma_i}{(M_i-W)^2+\frac{1}{4}\Gamma_i^2}\right)\,, \qquad (3.5)$$

where Γ_i is the total width of a resonance of mass M_i.

As is well known, there exists an alternative parametrization of inelastic e^--N scattering in terms of "scalar" and transverse parts of total photoabsorption cross sections for virtual photons, viz., $\sigma_S(W^2,k^2)$ and $\sigma_t(W^2,k^2)$.[36] The equivalence between these two modes of description is expressed by the following relations:

$$W_1=\frac{\varphi}{4\pi^2\alpha}\sigma_t\,, \qquad (3.6)$$

$$W_2=\frac{\varphi}{4\pi^2\alpha}\frac{k^2}{k^2+\nu^2}(\sigma_t+\sigma_S)\,, \qquad (3.7)$$

$$\varphi=(W^2-m^2)/2m\,. \qquad (3.8)$$

Another quantity of interest is the ratio R $(=\sigma_S/\sigma_t)$ which can be expressed in terms of structure functions W_1 and W_2 as[37]

$$R=\left(1+\frac{\nu^2}{k^2}\right)\frac{W_2}{W_1}-1\,. \qquad (3.9)$$

B. Photoabsorption

From the foregoing expressions for the total photoabsorption cross section for virtual photon scattering we can derive the corresponding results for real photon scattering by going to the limit $k^2\rightarrow 0$. In this limit, we have $\sigma_S(W^2,k^2)\rightarrow 0$ (since a real photon is transverse), and $\sigma_t(W^2,k^2)$ approaches the total photoabsorption cross section on the proton target. The generalization to a nucleon target is trivial through the use of the isospin operator τ_3 as indicated in Table II. It may, however, be noted that this quantity cannot strictly be regarded as the total photoabsorption cross section in the physical sense since one important ingredient for this purpose (the role of Pomeranchukon exchange) is not available in this model of s-channel resonance exchanges. It only includes

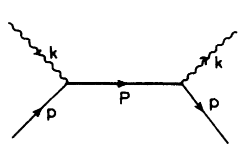

FIG. 2. Feynman diagram for the forward Compton scattering through exchange of spin-j state in the s channel.

the contribuiton of the Regge part of the total amplitude in the spirit of duality. Therefore it is not very meaningful in this model to compare separately the γp and γn cross sections with experiment despite the availability of such data. The best we can do is to calculate their difference, i.e., the quantity $\Delta\sigma_T$ $\{=[\sigma_T(\gamma p)-\sigma_T(\gamma n)]\}$ which is merely the isovector part (twice the coefficient of the τ_3 term) of the total photoabsorption cross section on a nucleon target, i.e., $\sigma_T(\gamma N)$.

To evaluate the isovector part of $\sigma_T(\gamma N)$ we have the essential simplification of having to consider only the N^* $(I=\frac{1}{2})$ resonances. The calculation can be done either by picking up the nucleonic contributions to the quantity $\sigma_t(W^2,k^2\rightarrow 0)$ of Eq. (3.6) or equivalently (and more simply) through a direct appeal to the Feynman diagrams of Fig. 2 through the use of the optical theorem

$$\sigma_T=\frac{1}{E_\gamma}\,\mathrm{Im}T_{ii}\,. \qquad (3.10)$$

Here E_γ is the energy of the incident photon in the laboratory system and $\mathrm{Im}T_{ii}$ is the imaginary part of the invariant Compton scattering amplitude in the forward direction, which can receive contributions only from the s channel (not u). The quantity T_{ii} may be evaluated directly in terms of the currents $j_\mu^{(\rho,\omega)}$ defined in Eq. (2.3) in the standard manner. Thus the contribution to T_{ii} from an N^* state of spin j is expressible as

$$T_{ii}=-\left(\frac{e}{g_\rho}\right)^2 e_\mu(k)e'_\mu(k)$$
$$\times\,\bar{u}(p)\langle(\tau_3 j_{\mu'}^{(\rho)}+\tfrac{1}{3}j_{\mu'}^{(\omega)})(\tau_3 j_\mu^{(\rho)\dagger}+\tfrac{1}{3}j_\mu^{(\omega)\dagger})\rangle\,u(p)\,, \qquad (3.11)$$

where e_μ is the (unit) polarization four-vector for the photon and the angular brackets $\langle\;\rangle$ imply the appearance of the propagator for the s-channel resonance. Further, the coefficient of $(\frac{1}{2}\tau_3)$ in (3.11), viz.,

$$\mathrm{Im}T_{ii}=-\tfrac{2}{3}\left(\frac{e}{g_\rho}\right)^2 e_\mu e_{\mu'}$$
$$\times\,\bar{u}(p)(\mathrm{Im}\langle j_{\mu'}^{(\rho)}j_\mu^{(\omega)\dagger}\rangle+\mathrm{Im}\langle j_{\mu'}^{(\omega)}j_\mu^{(\rho)\dagger}\rangle)u(p)\,, \qquad (3.12)$$

represents directly, *without further normalization*, the contribution from this resonance to $\Delta\sigma_T$. In Appendix B we indicate the method of evaluation for the contribution to (3.12) arising from a typical N_α resonance.

While, in principle, all the N-type states listed in Table II contribute to (3.12), the states N'_β and N_δ which correspond to relatively lower spins $(J=L-\frac{1}{2})$ make only nonleading contributions in the energy variable and hence are expected to be unimportant for the calculations. The actual numerical results are given in Sec. V B.

IV. OFF-MASS-SHELL EXTENSIONS

We now come to the more delicate question of extrapolation off the mass shell of the photon and the resonance. This extrapolation has to be made in two distinct areas, viz., the tensor $\xi_{\mu\nu}$ (including, in particular, the form factor) and the energy δ function. In our resonance formalism, the natural variables for extrapolation seem to be the quantities k^2 and M^2. In the absence of any strong theoretical guidelines we shall take a rather pragmatic view of this problem. Thus, so far as the square of the mass of the virtual photon is concerned, the replacement $\mu^2 \to -k^2$ appears to be the most natural thing to do, and indeed it was to implement this possibility in a mathematically meaningful manner (without having to face the danger of a sign flip in the denominator) that we had chosen the form given by Eq. (2.5). The problem of extrapolation in the mass M of the resonance is more tricky. The simplest choice which has already been considered with a fair amount of success in several two-body processes via s-channel exchanges is the replacement $M^2 \to W^2$.[15,16] In the present case, we would like to consider still another alternative for which we have really no good theoretical argument except for a desire to exploit the ambiguities in VMD extrapolations. Specifically, we shall consider as a simultaneous candidate the quantity

$$W_m^2 = m^2 + m_\rho^2 + 2m\nu$$

which agrees with W^2 on the ρ-meson mass shell and may thus be regarded as the square of the invariant mass of an $N\rho$ system (rather than $N\gamma$).

Actually a replacement of W^2 by W_m^2 makes little difference for *real* photoproduction processes, as may be seen from the results of the following paper on photoproduction of η or the results for real Compton scattering from nucleons evaluated in this paper. However, such a replacement would be much more sensitive for other processes, especially the process of electroproduction considered here, since extrapolation from the mass shell of a ρ meson to that of a virtual photon is too large. Since we are unable to defend the prescription $M^2 \to W_m^2$ on theoretical grounds, we have fallen back on a direct numerical comparison between the extrapolations

$$M^2 \to W^2 \quad \text{and} \quad M^2 \to W_m^2$$

in all the ingredients of the electroproduction cross sections. It turns out that while the difference between two assumptions is marginal for real photon scattering (which involves a "small" extrapolation) the numerical results of these two prescriptions for electroproduction differ widely from each other. Further, the numbers turn out to be such that the replacement of M^2 by W_m^2 in the most sensitive factors gives results closest to experiment, while the result of the replacement $M^2 \to W^2$ at these places is completely at variance with the data. The three most sensitive factors in the model are:

(i) the form factor of Eq. (2.5) where the resonance mass appears extensively;

(ii) the factor $\mathcal{G}_k^L$ which appears in $\xi_{\mu\nu}$ (see Appendix A);

(iii) the extended δ function (3.5), which involves the factor $1/2M$ [the main Breit-Wigner (B.W.) denominator must however remain untouched].

A vast numerical superiority is the only defense we have for using the empirical prescription $M^2 \to W_m^2$ at this stage in the hope that a more substantial justification would be eventually found for it if it indeed corresponds to any physical reality.

The extrapolation $M^2 \to W_m^2$ is still not adequate for the form factor which now takes the form

$$f_{LJ}^{(+)} = \left(\frac{2(W_m m)^{1/2} S_F(J)^{1/4}}{W_m^2 + m^2 + k^2}\right)^{L+1} \left(\frac{m_\rho}{m_\pi}\right)^{1/2} C_L^{(+)},$$

$$f_{LJ}^{(-)} = \left(\frac{2(W_m m)^{1/2} S_F(J)^{1/4}}{W_m^2 + m^2 + k^2}\right)^{L} \left(\frac{m_\rho}{m_\pi}\right)^{1/2} m_{A_1} C_L^{(-)}. \tag{4.1}$$

While this form is satisfactory for the first few resonances on the energy scale, it presents a formal problem of divergence arising out of a summation over an infinite series in the J variable which must be encountered for each type of trajectory. To overcome this formal difficulty we first make use of the linear relation between M^2 and J and then employ the prescription $M^2 \to W_m^2$ to finally obtain the effective replacement

$$(J)^{1/4} = (a'M^2 + b')^{1/4} \to (a'W_m^2 + b')^{1/4} \tag{4.2}$$

beyond the first few (2 or 3) recurrences of a given resonance type. This would imply that the modification (4.2) would affect essentially the continuum region but leave unaltered the predictions of the factor $(J)^{1/4}$ for the resonance region.

V. COMPARISON WITH EXPERIMENT

In this section, we shall describe our numerical results for both inelastic e^--N scattering and photoabsorption in relation to the experimental data. A more detailed comparison with contemporary models is relegated to the last section.

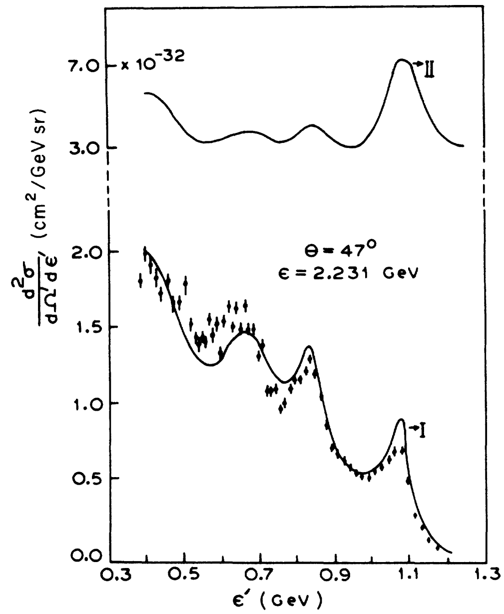

FIG. 3. Double differential cross section for inelastic $e^- - p$ scattering plotted against final electron energy ϵ' for fixed ϵ (= 2.231 GeV) and θ (= 47.0°) compared with the data (●) of Ref. 38. Curves I and II correspond to the prescriptions $(M^2 \rightarrow W_m^2)$ and $(M^2 \rightarrow W^2)$, respectively.

A. Inelastic e^--N Scattering

The experimental data for this process are characterized by the plot of the double-differential cross section $d^2\sigma/d\Omega' d\epsilon'$ versus ϵ' at constant values of ϵ and θ.[38-40] In order to facilitate the comparison with experimental data, it is better to divide the discussion of the data in terms of two energy zones, I and II, the data for which come

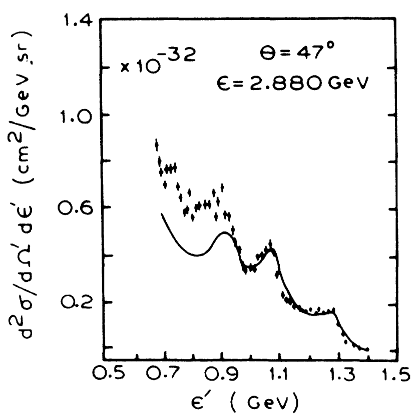

FIG. 4. Double differential cross section plotted against ϵ' for $\epsilon = 2.880$ GeV, and $\theta = 47.0°$. The data points are from Ref. 38. The theoretical curve (as in all the subsequent figures) is drawn corresponding to the prescription $(M^2 \rightarrow W_m^2)$ only.

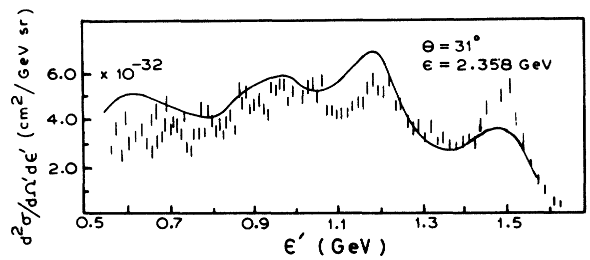

FIG. 5. Same as in Fig. 4 for the case of $\epsilon = 2.358$ GeV, $\theta = 31.0°$. The experimental points are from Ref. 39.

from quite distinct sources. Zone I, which we arbitrarily take to correspond to $\epsilon \lesssim 5.0$ GeV is characterized by the appearance of only resonance bumps in electroproduction, while zone II, which corresponds to $\epsilon \gtrsim 5.0$ GeV, has both the resonance electroproduction region and the continuum (i.e., $W > 2.0$ GeV).

The kind of plot that is experimentally available for the double-differential cross section as a function of ϵ' (for fixed θ) makes the dependence on k^2 rather implicit, though the latter can be inferred by analyzing for each resonance region the variation of the peak for different θ, ϵ values (which effectively amounts to variation with k^2). Attempts have been made by some experimentalists, notably Clegg,[41] to depict variations with k^2 directly for the three main resonance regions (which should, however, be distinguished from contributions from *individual* resonances). In accordance with our preference outlined in Ref. 15 for dealing directly with the raw data where available, rather than compare the predictions with "derived" data we prefer to confine our comparison to the ϵ' plots (for fixed θ and ϵ) of the double-differential cross section. Accordingly Figs. 3-6 give our plots for different θ and ϵ, together with the experimental data which are taken from the DESY[38] and Harvard[39] groups. These figures show that the more prominent bumps in the regions of $F_{37}(1940)$, $F_{15}(1690)$, $D_{13}(1520)$, and $P_{33}(1238)$ are well fitted by the calculated curves in accordance with the ansatz $M^2 \rightarrow W_m^2$ discussed in the previous section. For comparison, we have also indicated in one

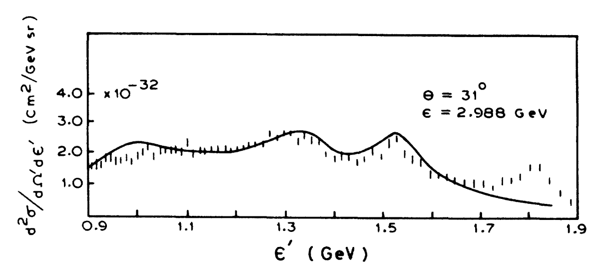

FIG. 6. Same as in Fig. 5 for the case of $\epsilon = 2.988$ GeV, $\theta = 31.0°$.

sample case the result of the alternative ansatz $M^2 \to W^2$ discussed in the previous section. Since the numerical contrast is too obvious to merit further comments, this fact was used as an empirical guiding principle for the considerations discussed in Sec. IV. The over-all fit to all the curves looks quite impressive, except for the P_{33} peak corresponding to $\epsilon = 2.988$ GeV and $\theta = 31°$.

Recently the electroproduction process has also been studied in the relativistic quark model by Ravndal[42] and Copley *et al.*[43] As noted by these authors, the relativistic quark model results in a substantial improvement over the corresponding nonrelativistic model.[6] Unfortunately, a direct comparison with their calculations has not been possible because of the emphasis in Ref. 42 on the variation of k^2 at individual resonance peaks. In our plots the inference of a reasonably accurate variation with k^2 is warranted indirectly through the agreement between the experimental and theoretical bumps for several (ϵ, θ) cases which incorporate a fairly wide variation with k^2 for each bump (e.g., for the bump corresponding to the P_{33} resonance, k^2 varies from 1.0 GeV^2 to 2.38 GeV^2). While our calculated curves include both the high-spin ($J = L + \frac{1}{2}$ and $J = L + \frac{3}{2}$) and low-spin ($J = L - \frac{1}{2}$) resonances, it turns out that the latter make negligible (<10%) contributions to the cross sections in this model, while the dominant contributions arise from summation over the N_α, N_γ, Δ_α, and Δ_δ trajectories. This leads us to infer that the three prominent peaks around W equaling 1.238, 1.520, and 1.690 GeV receive their dominant contributions from $P_{33}(1238)$, $D_{13}(1520)$, and $F_{15}(1690)$ resonances, respectively. This result seems to be somewhat at variance with that of Ref. 42 according to which, barring the P_{33} peak, each of the other resonance regions receives collective contributions of comparable magnitudes from more than one single resonance. However, to the extent

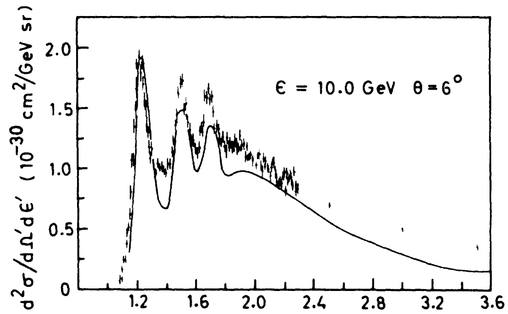

FIG. 8. Same as in Fig. 7 for the case of $\epsilon = 10.0$ GeV and $\theta = 6°$.

that both models (taken in their totality) seem to give comparable fits to the experimental data, it would appear difficult to discriminate between these two models on the basis of only electroproduction data in the resonance region. Perhaps a comparison in respect to several other processes would lead to a more meaningful discrimination between the two models.

We now come to the discussion of the energy zone II ($\epsilon \gtrsim 5.0$ GeV) for which most of the data are available from the SLAC-MIT collaboration.[40] As noted earlier, this zone receives contributions from both the resonances and the continuum. Figures 7, 8, and 9 show the dependence of our calculated cross sections for the incident energies of 7.0, 10.0, and 16.0 GeV, respectively, at small angle (6°), together with the corresponding experimental data. For the evaluation of the theoretical curves the numerical effect of summation over an infinite number of states turns out to be appreciably more important than in the previous region. (This is where the role of duality seems to be indicated, in a quantitative manner.) Here again the dominant contributions arise from the summation over the leading trajectories (N_α, N_γ, Δ_α, and Δ_δ)[44] while much smaller values (<5%) result from the other trajectories of $J = L - \frac{1}{2}$.

Figures 7 and 8 show that the data in both the resonance and continuum regions are well reproduced in our model for the incident energies 7.0

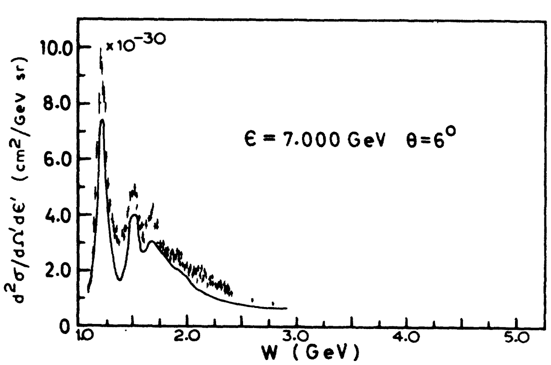

FIG. 7. Double-differential cross section plotted against the invariant missing mass W compared with the data of Ref. 40. The values of ϵ and θ in this case are 7.0 GeV and 6°, respectively.

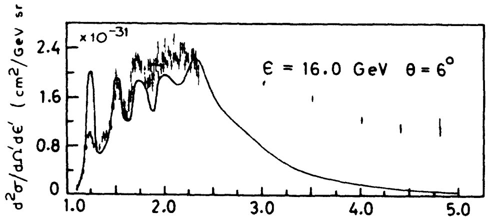

FIG. 9. Same as in Fig. 7 for the case of $\epsilon = 16.0$ GeV and $\theta = 6°$.

GeV and 10.0 GeV. An incident energy of about 10.0 GeV seems to be about the limit of validity of this model since the fits turn out to deteriorate progressively as the incident energy is increased; a typical curve is shown in Fig. 9 for $\epsilon = 16.0$ GeV. It is noticed that while the resonance region gives a tolerable fit even for this energy, the calculated curve falls appreciably short of the data points in the continuum region. This should not perhaps come as too much of a surprise, considering the problem of scaling that is involved in this region. Unfortunately our model does not satisfy the scaling condition for νW_2, being short of this requirement by a factor

$$\sim [m_\rho^2/(m_\rho^2 + k^2)]^2$$

which remains uncovered due to the lack of a compensating factor $\sim k^4$ in the numerator. A formal way to restore scaling would therefore be to supply a factor $\sim k^4$ in the numerator by exploiting an inherent ambiguity in VDM which has been recognized in the literature.[45] Specifically this may be achieved in our model by the replacement

$$\frac{em_\rho^2}{g_\rho(k^2+m_\rho^2)} \to \frac{-ek^2}{g_\rho(k^2+m_\rho^2)}, \tag{5.1}$$

which is certainly not incompatible with the overall VDM[45] spirit. However, it turns out that while scaling may be formally achieved for νW_2 with this prescription, the numerical values for this quantity are much too large in the resonance region which is characterized by relatively low values for the variable[9]

$$\omega' = 1 + \frac{W^2}{k^2} = \frac{2m\nu}{k^2} + \frac{m^2}{k^2}. \tag{5.2}$$

Even in the region of higher ω', the magnitude of νW_2 turns out to be about twice the experimental numbers.[9]

Finally, we have made some estimates of the quantity R $(=\sigma_S/\sigma_t)$ on the basis of our model and

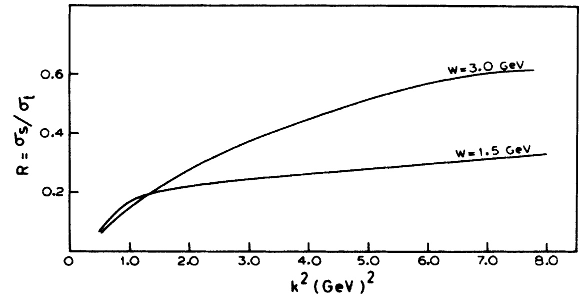

FIG. 10. Plot of ratio R against k^2 for fixed W. The two curves correspond to the cases of $W = 1.5$ GeV and $W = 3.0$ GeV, respectively.

this we have plotted in Fig. 10 as a function of k^2 for a few typical values of W. The numerical magnitude of R which ranges from ~0.05 to ~0.6 in this region seems to conform to the general belief that it is rather small on the whole, a result which is also predicted by the relativistic quark model.[43]

B. Results on Photoabsorption

In accordance with the ideas outlined in Sec. III B, we consider it desirable to record simultaneously the results of calculation of the $I = 1$ part of the photoabsorption cross section. Figure 11 shows these results for $\Delta\sigma_T$ together with the recent data.[46] The agreement between the calculated and the observed curves looks as good as can be expected from a comparison with the inadequately accurate data whose most important feature seems to be a slight preponderance of $\sigma_T(\gamma p)$ over $\sigma_T(\gamma n)$. The experimental trend of a general decrement in $\Delta\sigma_T$ with the incident photon energy is also reproduced by the model.

It is of interest to discuss the relative signs and magnitudes of the contributions to $\Delta\sigma_T$ arising from the different resonance towers. Numerically, the dominant contributors are the N_α, N_γ, and N_β'' trajectories, while the lower-lying trajectories N_β' and N_δ have been found to make negligible contribution. This is in harmony with the general ob-

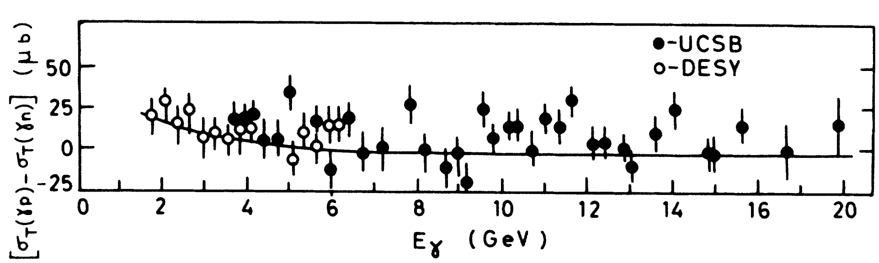

FIG. 11. Plot of the difference of total photoabsorption cross section on the proton and the neutron targets ($\Delta\sigma_T$) against the incident photon lab energy (E_γ). The experimental points are taken from Ref. 47.

servations made in Sec. III B regarding nonleading contributions from these low-lying states. As to the relative signs of the contributions, the N_α and N_γ trajectories tend to make $\Delta\sigma_T$ negative, while the N_β'' produces the opposite sign. Among the less important trajectories, only N_γ' (Ref. 47) makes $\Delta\sigma_T > 0$ while the others (N_β' and N_δ) give the opposite sign. The final pattern shown in Fig. 11 is the result of interference of all these effects.

It is also of interest to compare the above pattern of contributions to photoabsorption with the corresponding patterns for inelastic e^--p scattering as well as the n-p mass difference. This comparison is depicted in Table III which shows that while there is a considerable similarity between the roles of these resonances for inelastic e^--p scattering and photoabsorption, there is a much sharper difference between these two processes, on the one hand, and the result for n-p mass difference on the other. Thus we find that (i) the roles of the dominant contributors are interchanged and hence (ii) the relative signs of the contributions to the two processes are flipped. To the extent that both patterns are seemingly in accord with the respective data, it would be tempting to infer that there may well be a "causal connection" between the *positive* values for the quantity $\Delta\sigma_T$ on one hand and the *negative* value of $(\delta m_p - \delta m_n)$ on the other. And the above patterns (especially the sign pattern) do not appear to be entirely model-dependent. Take the case of N_α for example. The respective signs (opposite) of its contributions to $I=1$ part of the real γ-N scattering and the mass-difference calculations can be understood purely in terms of *algebraic structures* (*not* numerical values) of the corresponding amplitudes. The relative magnitudes of the different contributions to the two processes are of course more dynamical (model-dependent) in content. However, the main mechanism that seems to be operative here is the fact that in general the lower-spin ($J = L - \frac{1}{2}$) states tend to make themselves felt more through their "virtual" effects (in the calculation of electromagnetic masses, for example) than through their impact on "real" processes (e.g., γ-N scattering cross sections) which tend to pick up the higher-spin ($J = L + \frac{1}{2}$ and $J = L + \frac{3}{2}$) states for the dominant energy dependence. It would thus appear that the lower-spin states, which remain largely buried under the contributions of higher-J states in scattering processes (and hence are experimentally more difficult to detect), come up for a more prominant role in virtual processes such as those involved in the evaluation of the mass differences. From this point of view the inference of a sort of correlation between the positive value of $\Delta\sigma_T$ and the negative value of $(\delta m_p - \delta m_n)$ may not seem to be too optimistic. Details of the mass difference calculations, for which preliminary results were published earlier,[22] will be presented elsewhere.[48]

TABLE III. Comparison of the relative magnitudes and signs of the contributions of various towers to the three processes. For the calculations of $\Delta\sigma_T$ and $(\delta m_p - \delta m_n)$ the names of various towers have been written in the descending order of magnitude of their numerical contribution; further, the signs (±) denote the positive and negative contributions, respectively. The break after the fourth row denotes a major break in the magnitude of contribution; the towers listed below this break make a much smaller contribution than those listed above it.

Inelastic e^--N scattering	$\Delta\sigma_T$	$(\delta m_p - \delta m_n)$
N_α	N_β'' (+)	N_δ (−)
N_γ	N_α (−)	N_α (+)
Δ_α	N_γ (−)	N_β (−)
Δ_δ		N_γ (+)
N_γ'	N_β' (−)	N_γ' (+)
N_δ	N_γ' (+)	N_β' (−)
Δ_β	N_δ (−)	N_β'' (+)

Finally we note that the difference between the two prescriptions $M^2 \to W^2$ and $M^2 \to W_m^2$ in this case is only marginal, as in the case of photoproduction of η (AM). This is expected because a real photoabsorption process involves a much smaller extrapolation in the photon mass than does inelastic e^--N scattering (virtual-photon scattering).

VI. SUMMARY AND CONCLUSION

We have studied the problems of inelastic e^--N scattering and the photoabsorption in the framework of our model of higher baryon couplings. This model, which is applicable to high-energy processes in the spirit of duality through a sum over an infinite number of resonances (a facility for which is available in the model through a unified coupling structure for arbitrary spins), is found to reproduce the experimental results rather well for (i) inelastic e^--N scattering up to an incident electron energy of about 10 GeV (lab), (ii) the difference between the total photoabsorption cross sections on proton and neutron targets for the entire available range of data (up to the incident photon laboratory energy of 18.0 GeV), and (iii) the ratio $R = \sigma_S/\sigma_t$ which comes out to have a reasonably small magnitude in conformity with the general belief. For the electroproduction process, whereas all the characteristics of the resonance region turn out to be well described up to arbitrarily high energies, the property of scaling, which is a characteristic of the deep-inelastic region, is not found to be satisfied. The reproduction of the experimental results in the resonance electroproduction region and also the continuum region (the latter up to $\epsilon = 10.0$ GeV at least) may be regarded as a measure of support for the assumed power structure ($\sim x^l$) of the form factor as well as the general prescription of extrapolation ($M^2 \to s$) outlined in Sec. IV and in earlier references (Refs. 15 and 16). This result also supports the general observation of Bloom and Gilman[9] that resonances play an important part even in the high-energy region. The very good fits to the data for $\Delta\sigma_T$ suggest, in conformity with Ref. 9, that a substantial part of the $I=1$ amplitude of the forward Compton scattering amplitude is indeed saturated by s-channel resonances.

A serious drawback of our model lies in its failure to reproduce the continuum region at high energies despite the availability of the facilities for a formal application of the duality principle through a summation over an infinite number of resonances. One point of view would be to suppose, following Harari,[49] that a major part of the amplitude for virtual Compton scattering for large k^2 is contributed by the Pomeranchukon. However, the Bloom-Gilman[9] analysis of electroproduction data over a wide range of energies seems to suggest, with equal conviction, that resonances are able to account for scaling almost quantitatively. The recent resonance model of Domokos *et al.*[11] would also seem to warrant a similar conclusion. Unfortunately, we are not able to achieve scaling within our model while demanding a simultaneous fit to the resonance region. We have sought to compensate for this failure by providing a quality fit to the resonance region up to sufficiently high energies ($\epsilon = 16.0$ GeV), and even to the continuum region up to $\epsilon = 10.0$ GeV. This achievement may be contrasted with the performance of the model of Domokos *et al.* which does not fit the resonance region in detail, or with the Bloom-Gilman analysis according to which the fits to the resonance region are merely confined to an average description (no structure effects).

One possible clue to the understanding of this failure of our model in the higher-energy region (for $\epsilon > 10.0$ GeV), as also mentioned in AM (following paper), may lie in the role of daughters of successively lower ranks which presumably become progressively more important as the energy scale is increased. It is conceivable that a sum over these (infinite) sequences of daughters may increase the cross sections in the continuum region for higher energies to the level of the experimental data.[50] As yet, we do not see how to incorporate this feature of daughter trajectories in this model which must therefore pay the price of breaking down beyond a certain limit (up to $\epsilon \sim 10.0$ GeV in the present case) on the energy scale. A more detailed discussion of the pros and cons of the model is given in the following paper (AM).

ACKNOWLEDGMENT

One of us (S.K.S.) is grateful to the National Council of Educational Research and Training, New Delhi, for a research scholarship.

APPENDIX A

To illustrate the type of functions that arise, we indicate briefly the evaluation of the contribution for a typical resonance of spin $J = L + \frac{1}{2}$ for type-A coupling even at the cost of a little repetition with the existing literature. This will also help in bringing out some of the tricky extrapolation problems that are involved.

We start with the tensor $\xi_{\mu\nu}$ which in this case is

$$\xi_{\mu'\mu} = G^2\,\mathrm{Tr}\left[i\sigma_{\mu'\nu'}k_{\nu'}\,\Theta^{\nu_1\cdots\nu_L}_{\mu_1\cdots\mu_L}(L+\tfrac{1}{2},P)\, i\sigma_{\mu\nu}k_\nu \left(\frac{m - i\not{p}}{2m}\right)\right](k_{\mu_1})^L (k_{\nu_1})^L \,. \tag{A1}$$

The factor G is the product of three factors: the appropriate SU(6)×O(3) factors, the form factor $f^{(+)}_{LJ}$, and the factor $em_\rho^2/g_\rho(m_\rho^2 + k^2)$ arising out of VMD hypothesis. The projection operator $\theta^{(\nu)}_{(\mu)}(L+\frac{1}{2})$ for the baryon resonance of spin ($J = L + \frac{1}{2}$) has the form[51]

$$\Theta^{\nu_1\cdots\nu_L}_{\mu_1\cdots\mu_L}(L+\tfrac{1}{2},P) = \frac{M - i\not{p}}{2M}\left(\frac{L+1}{2L+3}\right)\gamma_{\mu_0}\gamma_{\nu_0}\Theta^{\nu_0\nu_1\cdots\nu_L}_{\mu_0\mu_1\cdots\mu_L}(L+1,P)\,, \tag{A2}$$

with the help of which Eq. (A1) is amenable to quick simplification and hence to the identification of ξ_1 and ξ_2 (as the coefficients of $\delta_{\mu\nu}$ and $p_\mu p_\nu$, respectively) in a straightforward way. Thus

$$\xi_1 = G^2\left(\frac{2(P\cdot k)^2}{Mm} + k^2 + k^2\frac{M}{m} - k^2\frac{P\cdot k}{Mm}\right)\frac{(L+1)!}{(2L+1)!!}\,\mathcal{G}_k{}^L\,,$$
$$\xi_2 = G^2\left(\frac{2k^2}{Mm}\right)\frac{(L+1)!}{(2L+1)!!}\,\mathcal{G}_k{}^L\,, \tag{A3}$$

where

$$\mathcal{G}_k = k_\mu \Theta_{\mu\nu} k_\nu = k^2 + \frac{(P\cdot k)^2}{M^2}\,, \tag{A4}$$

$\Theta_{\mu\nu}$ being the spin-1 projection operator.

The problem of extrapolation off the mass shell in the quantity $\mathcal{G}_k$ which appears in this expression rather sensitively (with a high exponent) is discussed in Sec. IV.

The contributions of other resonances to the functions ξ_1 and ξ_2 via different types of couplings can be written in a similar manner, apart from a lengthy but routine problem of algebraic complexity.

APPENDIX B

We indicate here the method of evaluation of $\mathrm{Im}T_{ii}$ for the case of a typical resonance contribution, say N_α, as an illustration of the computation techniques. The structure of the currents for the coupling to an N_α resonance is

$$j^{(\rho)}_{\mu'} = \bar\psi\left[\left(\tfrac{5}{3}i\sigma_{\mu'\nu'}k_{\nu'} + i\,m_\rho\gamma_{\mu'}\right)f^{(+)}_{LJ}(k_{\mu_1'})^L\psi^{L+1/2}_{\mu_1'\cdots\mu_L'} + f^{(-)}_{LJ}\tfrac{5}{3}\left(\frac{L}{2L+1}\right)^{1/2}\psi^{L+1/2}_{\mu'\mu_2'\cdots\mu_L'}(k_{\mu_2'})^{L-1}\right]\,,$$
$$j^{(\omega)}_{\mu'} = \bar\psi\left[\left(i\sigma_{\mu'\nu'}k_{\nu'} + 3i\,m_\rho\gamma_{\mu'}\right)f^{(+)}_{LJ}(k_{\mu_1'})^L\psi^{L+1/2}_{\mu_1'\cdots\mu_L'} + f^{(-)}_{LJ}\left(\frac{L}{2L+1}\right)^{1/2}\psi^{L+1/2}_{\mu'\mu_2'\cdots\mu_L'}(k_{\mu_2'})^{L-1}\right]\,, \tag{B1}$$

where the form factors $f^{(\pm)}_{LJ}$ refer to the direct and recoil term, respectively. Substitution of this expression in (3.12) leads to the consideration of the following different types of tensors (orders 2, 1, and 0) as a result of contraction of the projection operator $\Theta^{(\mu')}_{(\mu)}$ with different numbers of available four-vectors $(k_\mu, k_{\mu'})$:

$$\Phi^{\mu'}_{\mu} = (k_{\mu_2'}\cdots k_{\mu_L'})\gamma_{\bar\mu'}\gamma_{\bar\mu}\,\Theta^{\bar\mu'\mu'\mu_2'\cdots\mu_L'}_{\bar\mu\mu\mu_2\cdots\mu_L}(k_{\mu_2}\cdots k_{\mu_L})$$
$$= \frac{\mathcal{G}_k{}^{L-2}(L-1)!(L+1)}{2(2L+1)!!}\left[\mathcal{G}_k(L+1)\Theta_{\mu\mu'} + V_\mu V_{\mu'}(L-1) - i\hat\sigma_{\mu'\mu}\mathcal{G}_k + iV_\lambda(V_{\mu'}\hat\sigma_{\mu\lambda} - V_\mu\hat\sigma_{\mu'\lambda})(L-1)\right], \tag{B2}$$

where

$$\Theta_{\mu\mu'} = \delta_{\mu\mu'} + \frac{P_\mu P_{\mu'}}{M^2}\,, \qquad V_\mu = k_{\mu'}\Theta_{\mu\mu'} = k_\mu + \frac{P\cdot k\,P_\mu}{M^2}\,,$$

$$\hat\sigma_{\mu\nu} = \frac{1}{2i}(\hat\gamma_\mu\hat\gamma_\nu - \hat\gamma_\nu\hat\gamma_\mu)\,, \qquad \hat\gamma_\mu = \gamma_{\mu'}\Theta_{\mu\mu'} = \gamma_\mu + \frac{\not P P_\mu}{M^2}\,,$$

$$\Phi_\mu = \Phi^{\mu'}_{\mu}k_{\mu'} = \frac{\mathcal{G}_k{}^{L-1}(L+1)!}{(2L+1)!!}\left(V_{\mu'} + \tfrac{1}{2}i\hat\sigma_{\mu'\lambda}V_\lambda\right), \tag{B3}$$

$$\Phi^{\mu'} = \Phi^{\mu'}_{\mu}k_\mu = \frac{\mathcal{G}_k{}^{L-1}(L+1)!}{(2L+1)!!}\left(V_{\mu'} - \tfrac{1}{2}i\hat\sigma_{\mu'\lambda}V_\lambda\right), \tag{B4}$$

$$\Phi = \Phi^{\mu'}_{\mu}k_\mu k_{\mu'} = \frac{\mathcal{G}_k^L(L+1)!}{(2L+1)!!}\,. \tag{B5}$$

In terms of these symbols the actual expression for the N_α contribution to Eq. (3.12) works out in a straightforward manner as

$$\operatorname{Im} T_{ii} = -\tfrac{2}{3}\left(\frac{e}{g\rho}\right)^2 e_\mu e_{\mu'} \bar{u}(p)\Bigg\{(\tfrac{5}{3} i\sigma_{\mu'\nu'}k_{\nu'} + i m_\rho \gamma_{\mu'})(M - i\not{P})(-i\sigma_{\mu\nu}k_\nu + 3 i m_\rho \gamma_\mu)(f_{LJ}^{(+)})^2 \Phi$$

$$+ (\tfrac{5}{3} i\sigma_{\mu'\nu'}k_{\nu'} + i m_\rho \gamma_{\mu'})(M - i\not{P})\Phi_\mu \left[f_{LJ}^{(+)} f_{LJ}^{(-)} \left(\frac{L}{2L+1}\right)^{1/2}\right]$$

$$+ (i\sigma_{\mu'\nu'}k_{\nu'} + 3 i m_\rho \gamma_{\mu'})(M - i\not{P})\Phi \left[f_{LJ}^{(+)} f_{LJ}^{(-)} \frac{5}{3}\left(\frac{L}{2L+1}\right)^{1/2}\right]$$

$$+ (M - i\not{P})\Phi^{\mu'}(-i\sigma_{\mu\nu}k_\nu + 3 i m_\rho \gamma_\mu)\left[f_{LJ}^{(+)} f_{LJ}^{(-)} \frac{5}{3}\left(\frac{L}{2L+1}\right)^{1/2}\right]$$

$$+ (M - i\not{P})\Phi^{\mu'}(-\tfrac{5}{3} i\sigma_{\mu\nu}k_\nu + i m_\rho \gamma_\mu)\left[f_{LJ}^{(+)} f_{LJ}^{(-)} \frac{5}{3}\left(\frac{L}{2L+1}\right)^{1/2}\right]$$

$$+ 2(M - i\not{P})\Phi_\mu^{\mu'}(f_{LJ}^{(-)})^2 \left(\frac{L}{2L+1}\right)\Bigg\} u(p)\pi\delta(P^2 + M^2)\left(\frac{2j+1}{4j+4}\right). \qquad \text{(B6)}$$

The treatment of the δ function proceeds on identical lines to those described in Eq. (3.5) of the text.

This expression can be simplified through the use of the relations

$$k^2 = 0, \quad e^2 = 1, \quad P\cdot e = p\cdot e = k\cdot e = 0,$$

and (B7)

$$\bar{u}(p)\not{P}u(p) = \frac{P\cdot p}{m}, \quad \bar{u}(p)i\not{k}u(p) = \frac{p\cdot k}{m}, \quad \bar{u}(p)\not{P}\not{k}u(p) = \bar{u}(p)\not{k}\not{P}u(p) = p\cdot k,$$

eventually leading to an expression depending only on the Lorentz-invariant quantity $p\cdot k$ $(= -mE_\gamma)$.

Exactly similar considerations apply to the N_γ resonances. The $N_\beta'{}'$ resonance involves a considerably greater amount of algebra but no essentially new difficulty.

---

[1]K. Igi and S. Matsuda, Phys. Rev. Letters 18, 625 (1967).

[2]A. Logunov, L. D. Soloviev, and A. N. Tavkhelidze, Phys. Letters 24B, 181 (1967).

[3]R. Dolen, D. Horn, and C. Schmid, Phys. Rev. 166, 1768 (1968).

[4]G. F. Chew and A. Pignotti, Phys. Rev. Letters 20, 1078 (1968).

[5]J. D. Jackson, Rev. Mod. Phys. 42, 12 (1970).

[6]N. S. Thornber, Phys. Rev. 169, 1096 (1968).

[7]J. D. Bjorken, Phys. Rev. 179, 1547 (1969).

[8]J. D. Bjorken and E. A. Paschos, Phys. Rev. 185, 1975 (1969).

[9]E. D. Bloom and F. J. Gilman, Phys. Rev. D 4, 2901 (1971).

[10]R. P. Feynman, M. Kislinger, and F. Ravndal, Phys. Rev. D 3, 2706 (1971); F. Ravndal, *ibid.* 4, 1466 (1971).

[11]G. Domokos, S. Kovesi-Domokos, and E. Schonberg, Phys. Rev. D 3, 1184 (1971).

[12]See, e.g., M. Pavkovic, Ann. Phys. (N.Y.) 62, 1 (1971).

[13]D. L. Katyal and A. N. Mitra, Phys. Rev. D 1, 338 (1970).

[14]D. K. Chaudhury and A. N. Mitra, Phys. Rev. D 1, 351 (1970).

[15]R. Mehrotra and A. N. Mitra, Phys. Rev. D 4, 1409 (1971).

[16]See S. A. S. Ahmed and A. N. Mitra, following paper, Phys. Rev. D 7, 2125 (1973), hereafter referred to as AM.

[17]K. Sen Gupta and V. K. Gupta, Phys. Rev. D 5, 1824 (1972).

[18]H. J. Lipkin and S. Meshkov, Phys. Rev. Letters 14, 670 (1965).

[19]A. N. Mitra, in *Lectures in High Energy Theoretical Physics*, edited by H. H. Aly (Gordon and Breach, London, 1970).

[20]A. N. Mitra, Ann. Phys. (N.Y.) 67, 578 (1971).

[21]D. K. Chaudhury, D. L. Katyal, and A. N. Mitra, Lett. Nuovo Cimento 2, 265 (1971).

[22]D. K. Chaudhury and A. N. Mitra, Phys. Letters 32B, 619 (1970).

[23]J. D. Bjorken and J. D. Walecka, Ann. Phys. (N.Y.) 38, 35 (1966).

[24]A. N. Mitra, Nuovo Cimento 61A, 344 (1969); 64A, 603 (1969).

[25]A. N. Mitra, Nuovo Cimento 56A, 1164 (1968).

[26]H. Harari, Rapporteur's talk, in *Proceedings of the Fourteenth International Conference on High Energy Physics, Vienna, 1968*, edited by J. Prentki and J. Steinberger (CERN, Geneva, 1968).

[27]R. R. Crittenden, R. M. Heinz, D. B. Lichtenberg, and E. Predazzi, Phys. Rev. D 1, 169 (1970).

[28] For the notation see Ref. 16.

[29] J. Schwinger, Phys. Rev. Letters 18, 923 (1967).

[30] The V-meson mass, which appears only in the type-B coupling via the structure of the meson matrix, has been put in for the sake of uniformity in dimensions among the "main" coupling structures in this problem (A, B, D).

[31] J. J. Sakurai, Ann. Phys. (N.Y.) 11, 1 (1960); M. Gell-Mann, Phys. Rev. 125, 1067 (1962).

[32] S. A. S. Ahmed, Phys. Rev. D 4, 2094 (1971).

[33] D. K. Choudhury, Oxford University report, 1971 (unpublished); Lett. Nuovo Cimento 2, 895 (1971).

[34] The form $M^2+m^2-\mu^2$, with its extrapolation $M^2+m^2+k^2$, also provides a formally valid application to the evaluation of electromagnetic masses without having to encounter the problem of unphysical poles in the energy plane of the virtual photon.

[35] R. Von Gehlen, Phys. Rev. 118, 1455 (1960); M. Gourdin, Nuovo Cimento 21, 1094 (1961).

[36] L. N. Hand, Phys. Rev. 129, 1834 (1963); F. J. Gilman, *ibid.* 167, 1365 (1968).

[37] R. E. Taylor, SLAC Report No. SLAC-PUB-677, 1969 (unpublished).

[38] L. Hand, in *Proceedings of the Third International Symposium on Electron and Photon Interactions at High Energies, Stanford, Calif., 1967* (Clearing House of Federal Scientific and Technical Information, Washington, D. C., 1968).

[39] A. A. Cone *et al.*, Phys. Rev. 156, 1490 (1967); 163, 1854(E) (1967).

[40] E. D. Bloom *et al.*, Phys. Rev. Letters 23, 930 (1969).

[41] R. L. Walker, in *Fourth International Symposium on Electron and Photon Interactions at High Energies, Liverpool, 1969,* edited by D. W. Braben and R. E. Rand (Daresbury Nuclear Physics Laboratory, Daresbury, Lancashire, England, 1970).

[42] F. Ravndal, Phys. Rev. D 4, 1466 (1971).

[43] L. A. Copley, G. Karl, and E. Obryk, Phys. Rev. D 4, 2844 (1971).

[44] The contribution for N_β'' vanishes for electron scattering off protons, since the $\bar{D}_{15}p\gamma$ coupling vanishes via the Moorhouse selection rule [see R. G. Moorhouse, Phys. Rev. Letters 16, 772 (1966)] which in this model corresponds to $m_\rho \approx m_\omega$ (Ref. 15). The $\bar{D}_{15}n\gamma$ coupling is nonzero, however.

[45] S. G. Brown, Phys. Rev. D 1, 207 (1970).

[46] *Proceedings of the International Symposium on Electron and Photon Interactions at High Energy, 1971,* edited by N. B. Mistry (Cornell Univ. Press, Ithaca, N. Y., 1972).

[47] The reason why N_γ and N_γ' produce opposite signs is simple: The former involves A-, B-, and E-type couplings simultaneously, while in the latter the types B and E are absent.

[48] D. K. Chaudhury *et al.* (unpublished).

[49] H. Harari, Phys. Rev. Letters 22, 1078 (1969).

[50] We understand that in the case of electroproduction, the importance of daughters in producing a satisfactory high-energy behavior has also been demonstrated recently by H. Goldberg [Northeastern Univ. report, 1972 (unpublished)].

[51] C. Fronsdal, Nuovo Cimento Suppl. 9, 416 (1958); R. Blankenbecler and R. L. Sugar, Phys. Rev. 168, 1597 (1968).

PHYSICAL REVIEW D VOLUME 7, NUMBER 7 1 APRIL 1973

Pionic and Electromagnetic Production of η in a Model of Higher Baryon Couplings

S. A. S. Ahmed and A. N. Mitra

Department of Physics and Astrophysics, University of Delhi, Delhi, India

(Received 20 July 1972)

An s-channel analysis of η-production processes induced by pions and photons on protons is made in the momentum region 2.9–13.3 GeV/c. The analysis is carried out in a model of higher baryon couplings, which is characterized by a relativistic extension of a broken $SU_6 \otimes O_3$ with partial symmetry scheme for $\bar{B}B_LP$ and $\bar{B}B_LV$ couplings in a unified fashion. In this high-energy extension of the model we incorporate seven baryon trajectories, viz., $N_\alpha(938)$, $N_\beta(1530)$, $N_\beta'(1715)$, $N_\beta''(1675)$, $N_\gamma(1520)$, $N_\gamma'(1675)$, and $N_\delta(1860)$, for which we carry out piecewise summations over the contributions of the particles involved in the corresponding towers, formally up to infinity. The predictions of the theory are compared with experiment with respect to the (i) total and differential cross sections and the recoil neutron polarization for the process $\pi^-p \to \eta n$, and (ii) differential cross sections for the process $\gamma p \to \eta p$ at several incident energies. In general the agreement with experiment is rather good up to $\sim$10 GeV/c. The reasons for the success up to this momentum, as well as the limitations to extension beyond this value, are discussed in the context of contemporary ideas.

I. INTRODUCTION

Because of the peculiar quantum numbers of the η meson which forbid its couplings to several meson pairs, a study of the production of this particle in πN and γN processes provides a unique opportunity to examine the working of duality in a relatively clean fashion. From the point of view